buildings

MDPI

Article

A Comparative Study of Machine Learning and Conventional Techniques in Predicting Compressive Strength of Concrete with Eggshell and Glass Powder Additives

Yan Gao [1,*] and Ruihan Ma [2]

[1] Civil, Environmental and Geomatic Engineering, University College London, London WC1E 6BT, UK
[2] School of Civil and Environmental Engineering, Nanyang Technological University, Singapore 639798, Singapore; maru0004@e.ntu.edu.sg
* Correspondence: ucesyga@ucl.ac.uk

Abstract: Recent research has focused on assessing the effectiveness of response surface methodology (RSM), a non-machine learning technique, and artificial neural networks (ANN), a machine learning approach, for predicting concrete performance. This research aims to predict and simulate the compressive strength of concrete that replaces cement and fine aggregate with waste materials such as eggshell powder (ESP) and waste glass powder (WGP) for sustainable construction materials. In order to ensure concrete's durability and structural integrity, a compressive strength evaluation is essential. Precise predictions maximize efficiency and advance sustainability, particularly when dealing with waste materials like ESP and WGP. The response surface methodology (RSM) and artificial neural network (ANN) techniques are used to accomplish this for practical applications in the built environment. A dataset comprising previously published research was used to assess ANN and RSM's predictive and generalization abilities. To model and improve the model, ANN used seven independent variables, while three variables, cement, waste glass powder, and eggshell powder, improved the RSM. Both the ANN and RSM techniques are effective instruments for predicting compressive strength, according to the statistical results, which include mean squared error (MSE), determination coefficient (R^2), and adjusted coefficient (R^2 adj). RSM was able to achieve the R^2 by 0.8729 and 0.7532 for compressive strength, while the accuracy of the results for ANN was 0.907 and 0.956 for compressive strength. Moreover, the correlation between ANN and RSM models and experimental data is high. The artificial neural network model, however, exhibits superior accuracy.

Keywords: artificial neural networks; response surface methodology; waste materials in concrete; eggshell powder; waste glass powder; compressive strength

Citation: Gao, Y.; Ma, R. A Comparative Study of Machine Learning and Conventional Techniques in Predicting Compressive Strength of Concrete with Eggshell and Glass Powder Additives. *Buildings* **2024**, *14*, 2956. https://doi.org/10.3390/buildings14092956

Academic Editor: Grzegorz Ludwik Golewski

Received: 16 August 2024
Revised: 5 September 2024
Accepted: 14 September 2024
Published: 19 September 2024

1. Introduction

For a long time, there have been serious concerns regarding CO_2 emissions [1]. Cement is a fundamental building ingredient and its production can result in significant CO_2 emissions [2]. Therefore, it is critical to look for innovative ways to fulfill the objective of low-carbon development [3]. Prior research has indicated that mixing various waste materials into construction materials might effectively lower CO_2 emissions [4–6]. When producing concrete mix, a variety of components are mixed with water and additives, including cement, coarse aggregate, and fine aggregate [7]. The use of a lot of cement, together with oxides of sulfur and nitrogen, significantly contributes to greenhouse gas emissions (about 7% of global emissions). The production of 1000 g of cement releases 90 g of CO_2 into the atmosphere [2,8]. In the modern day, researchers are becoming more interested in recycling waste materials due to the increasing demand for aggregates and cement in concrete and the need to preserve natural resources in an environmentally responsible manner [9].

Numerous trash dumps in open areas disperse infectious germs throughout our atmosphere and pollute the ecology [10]. The organic component causes the eggshell to become toxic. It is impacted by rats and worms, which become a public health hazard [11]. Eggshell trash is one type of solid waste that can be found in bakeries, factories, homes, poultry farms, and egg-laying farms, among other places [12]. In place of limestone, an eggshell has 94% calcium carbonate ($CaCO_3$), 1% calcium phosphate ($Ca_3(PO_4)_2$), 1% magnesium carbonate ($MgCO_3$), and 4% organic content [13–16]. Eggshell powder (ESP) shares a chemical composition with limestone [17]. When ESP is used in place of cement, the hydration process is accelerated and early compressive strength is provided in the form of better mechanical properties. The hard outer shell of an egg, known as an eggshell, is one kind of agricultural waste. Because egg production has been steadily rising globally, it is anticipated that the annual production of eggshells will exceed 8 million tons [12]. The chemical component calcium carbonate ($CaCO_3$), which is essential to the composition of eggshells, is needed for the development of calcium-silicate-hydrate (C-S-H) gel in cementitious composites [18]. For this reason, part of the cement and fine aggregate in building materials can be substituted using waste eggshell powder (WEP) [12].

Apart from ESP, the non-biodegradable nature of waste glass powder (WGP) also leads to serious environmental issues [19]. The severity of the growing WGP pollution in the ecosystem, including in the water and soil, is made worse by the lack of landfills for it. Recycling WGP is therefore an appropriate way to lessen the environmental problem [20,21]. In our daily lives, WGP is quite prevalent. It is present in many different products, including windows, bottles, and lightbulbs, all of which have a limited lifespan and should be reused in order to prevent the environmental problems associated with landfilling and stockpiling [22]. According to the standard ASTM C618-19, when waste glass is finely ground into powder, it is considered a pozzolanic or cementitious material since it contains a significant amount of silicon, calcium, and amorphous structure [23]. The mechanical impact of WGP as a cement substitute was examined in earlier research. WGP was substituted for OPC as supplemental cementitious material (SCM) up to a weight percentage of 25%, and its mechanical and physical characteristics were examined [24]. The findings demonstrated that WGP enhanced the mortar's absorption, tensile strength, and compressive strength, and decreased the density and void ratio. As a result, it can be said that WGP may be used to partially replace OPC.

Testing concrete in a lab to determine its strength requires a significant consumption of time and money [25]. Several factors could impact the strength of concrete even when it has ESP and WGP. Artificial neural networks (ANN), response surface methodology (RSM), and other machine learning approaches are now frequently utilized for predicting various scientific challenges [26]. For a long time, machine learning techniques have been used to forecast the performance of different parameters. But in recent years, its application in civil engineering has grown significantly [27]. Artificial neural networks (ANN) are one of the most often used approaches among the several ML-based solution types. Without taking into account explicit mathematical equations, the ANN can reliably find and learn underlying correlations between input and output data [28]. Furthermore, regardless of assumptions regarding mathematical models, ANN-based solutions are seen as a viable substitute for conventional statistical analytic techniques for function approximation and data fitting [29]. This kind of technique has also been used to determine the constituent properties of concrete materials. For example, it has been used to determine the nanoscopic elastic modulus of various cementitious matrix phases [30] and the abrasion performance of a geopolymer based on fly ash [31]. Additionally, numerous researchers explored how carbon nanotubes affect the mechanical characteristics of novel cement compositions using the ANN approach [32]. An input layer, one or more hidden layers, and an output layer make up an ANN [33]. Although ANNs may forecast more accurately than other statistical models, they are susceptible to local optimization as opposed to global optimization, just like other classical optimization techniques [34].

A thorough mathematical and statistical technique for modeling and assessing experimental problems is the response surface method (RSM) [35]. Multiple simultaneously varying factors are fitted to a quadratic function in RSM [36]. Compared to the laborious one-element-at-a-time strategy, which also ignores the interactions between factors, RSM provides a number of advantages for optimization [37]. RSM uses a mathematical model to forecast the desired qualities by proportioning the constituent materials to create an ideal blend [38]. This method is frequently used for experiment design and optimization, but its application in the concrete industry is very limited [39]. Moreover, RSM has been used in different studies on cement and concrete [40–42], but it has not been used much with concrete that has WGP and ESP. Therefore, the primary focus of this study is on applying RSM to forecast and optimize the compressive strength of ESP and WGP concrete. Lately, there has been an increase in interest among researchers in investigating the suitability of ANN machine learning modeling techniques and RSM (non-machine learning technique) for identifying practical solutions to problems. In order to compare the impacts of eggshell powder and recycled waste glass on concrete compressive strength, this study uses RSM and ANN to substitute cement and fine aggregate partially. In this study, ANN and RSM models were constructed using experimental data. The statistical measurements of mean square error (MSE), coefficient of determination (R^2), and correlation coefficient (R) were used to assess and compare the accuracy of the created models. To the best of the authors' knowledge, this is the first study to compare RSM with ANN for the purpose of forecasting mechanical qualities, including waste materials like eggshell powder and recycled waste glass.

2. Methodology

The study incorporates key parameters, ANN and RSM models, and dataset selections from earlier studies. MATLAB's Artificial Neural Fitting and Design Expert's central composite design were utilized to create input–target variable relationships in order to generate the prediction model. To ensure the model's reliability, datasets from the literature were employed. Engineering judgment was utilized to eliminate jumbled entries brought on by human error and improve dataset quality. Using R, R^2, and MSE, the prediction model's performance was assessed. These metrics offer a comprehensive assessment of the prediction ability and accuracy of the model. The impact of significant input elements on the prediction of concrete compressive strength was examined using a thorough parametric analysis. The purpose of this approach is to clarify the relative importance of the constituents of concrete strength.

2.1. Selection of Dataset

Creating accurate predictive models requires a dependable and complete dataset. This study used a complete literature review to collect data from previous research. Dataset acquisition was complicated by concrete compressive strength modeling. This analysis included data from 225 concrete examples from previous research [43,44]. Cement (kg/m^3), fine aggregate (kg/m^3), water (kg/m^3), Silica fume (kg/m^3), superplasticizer (kg/m^3), eggshell powder (kg/m^3), waste glass powder (kg/m^3), and compressive strength (MPa) are the inputs and outputs of this model.

2.2. Artificial Neural Network (ANN)

ANNs are built upon the concept of biological neural networks. Artificial neural networks (ANNs) are highly efficient methods for forecasting, grouping, identifying, and organizing data [44,45]. Their learning capabilities from training data are excellent and serve as "black boxes." As shown in Figure 1, a basic neural network is composed of an input layer that takes in input variables and an output layer that produces output signals. Hidden layers are sometimes defined as the layers that sit between the input and output layers. Selecting the right hidden layer is essential because too many hidden layers cause the model to overfit, while too few hidden layers cause the model to underfit [46]. In

addition, the presence of additional hidden layers in the model leads to an increase in the estimation time [47]. The intermediate computations that determine the neural network's output value are carried out by the hidden neurons that make up the hidden layers. Table 1 describes the statistical features of the data. The synaptic weight (w_i) is multiplied by each input (x_i). During the learning process, the weights are adjusted to obtain a certain level of accuracy. Applying bias, hidden layer neurons compute the weighted sum of the incoming signals (b). Bias is eliminated when there is insufficient meaningful input data, enabling the neuron to modify output independent of input values. Y is output following the transmission of the total through the activation function (f):

$$Y = f\left(\sum w_i * x_i + bni\right) \quad (1)$$

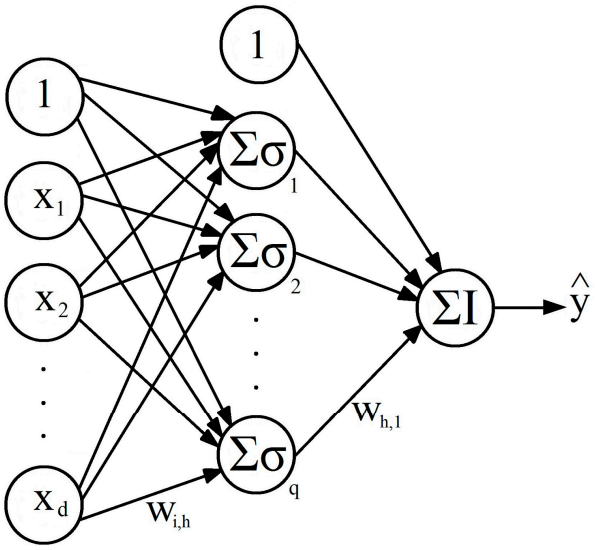

Figure 1. Single-layer neural network [48].

Table 1. Statistical summary of input and output parameters.

	Input Parameters		Output Parameter
	ESP	**WGP**	**Compressive Strength**
Statistical indicators	kg/m^3	kg/m^3	MPa
Minimum value	0.00	0.00	29.70
Mean value	32.06	32.06	44.65
Maximum value	121.50	121.50	64.98
Standard Deviation	40.46	40.46	6.77

Since the learning algorithm is the quickest method for training small feedforward neural networks, it was incorporated into the ANN model [49,50]. Additionally, in supervised learning scenarios, such as the ones in our study, it is the main response. The sigmoid activation function is often used in research [51]. The algorithm computes the variance between the expected and actual values. Adjusting weights and bias using the learning process sends the error back to the network [52].

2.3. Response Surface Methodology (RSM)

In RSM, independent variables (input parameters) interact with one or more responses (output parameters). It may estimate output parameters and produce a precise model with less experimental data [53]. This strategy is used when multiple variables affect the response. For each response, this study generated a central composite design (CCD) model, an RSM experimental design for second-order (quadratic) model prediction. The complete

methodology employed in this investigation is visually depicted in Figure 2. Furthermore, Table 2 presents the factors and their respective ranges of variation.

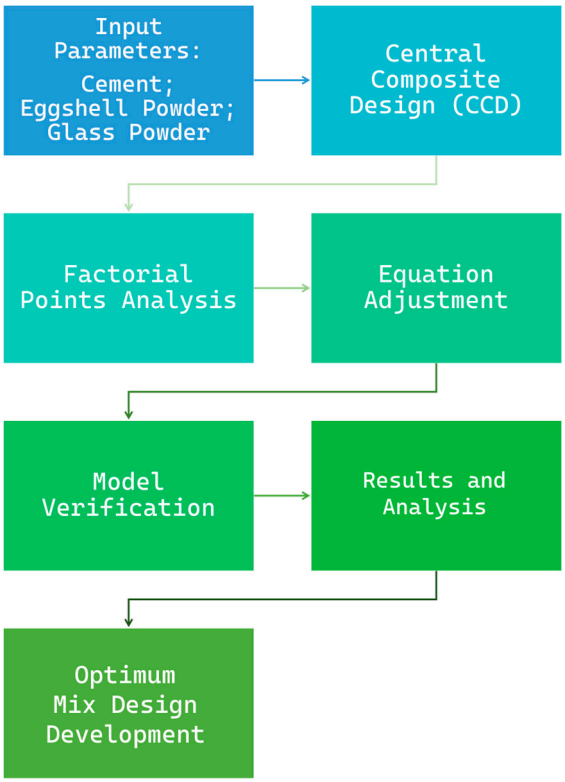

Figure 2. RSM Methodology.

The DESIGN EXPERT software (v11) was utilized to perform CCD data analysis and accomplish multi-variable optimization. The number of experiments is determined using Equation (2).

$$N = 2^K + 2K + C \quad (2)$$

where k, 2 k, and C were explained [53]. The center, axial, and factorial points are shown by CCD in Figure 3. Based on Equation (2), a total of 13 experimental points were recommended for the study. These points consisted of 5 factorial points without replication (2k), 4 axial points without replication (2k), and 1 center point with 4 replications (c).

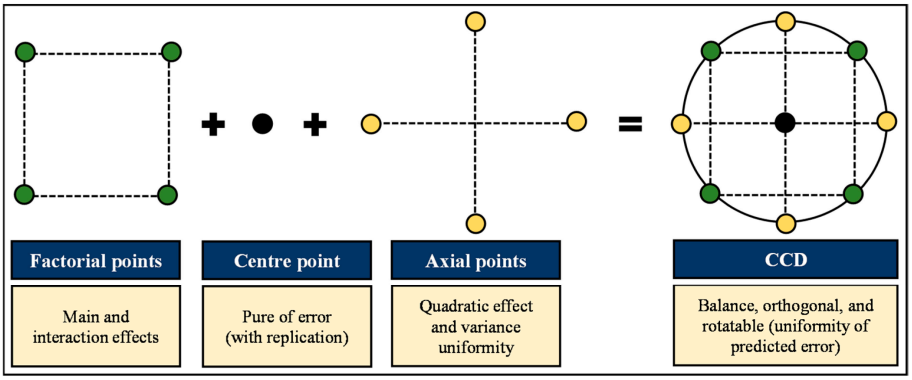

Figure 3. Illustration of factorial, center, and axial points in a central composite design (CCD) [54].

The best response was ascertained by applying the quadratic model or second-order polynomial in Equation (3).

$$y = \beta_0 + \sum \beta_i x_i + \sum \beta_{ii} x_i^2 + \sum \beta_{ii} x_i x_j \quad (3)$$

where y is the anticipated response value, β_0 is the intercept of the model, β_i represents the linear coefficients, β_{ii} refers to quadratic coefficients, and β_{ii} are coefficients of the variables' interaction. x_i and x_j are the independent variables [35].

Table 2. Compressive strength factor levels for RSM.

Factors	Response	Code	Factors Level of Code		
			Intermediate Level 0	High Level +1	Low Level −1
Cement (kg/m^3)	1	A	749.25	810	688.5
w/c	1	B	0.2727	0.2948	0.2506
Cement (kg/m^3)	2	A	728	810	646
ESP (kg/m^3)	2	B	50.75	121.5	0
Cement (kg/m^3)	3	A	686	760	612
ESP (kg/m^3)	3	B	54	108	0
Cement (kg/m^3)	4	A	728	810	646
WGP (kg/m^3)	4	B	70.25	121.5	19

3. Results and Discussion

3.1. Predicting Compressive Strength Using RSM

The CCD model was used in this study for analyzing six responses in compressive strength, which included cement, water/cement, ESP, and WGP as a variable. In Table 3 you can see the responses for 225 different mix designs. The regression coefficient, which indicates the direction of the association between a predictor and the response variable, and the *p*-value were two statistical criteria that were examined in an analysis of variance (ANOVA) [27]. ANOVA is a suitable statistical method for investigating the relationship between responses and changes, much like regression. The results indicate that the correlation coefficient values for some responses are above 90%, which is deemed satisfactory. As a 3D view, response 1's compressive strength, contour graph, predicted vs. actual results, and perturbation are shown in Figure 4.

The equations generated from Equation (4) were used to calculate the mathematical prediction of compressive strength for response 1.

$$C.S\ for\ response\ 1 = 47.07 + 2.99\ A - 2.06\ B - 0.3475\ AB - 8.58\ A^2 - 0.3607\ B^2 \quad (4)$$

where A and B represent the variables (cement and water/cement).

The model's F-value of 105.03 indicates that the model is statistically significant. The probability of an F-value of this magnitude occurring solely due to noise is only 0.01%. The *p*-value was 0.0001 less than 0.0500 indicates the model's terms are significant [55]. It is noteworthy that A, B, and A^2 hold considerable importance as model terms. Values beyond 0.1000 suggest that the model's terms lack significance. As shown in Figure 4a, the highest compressive strength predicted was 49.08 MPa at a cement content of 761 kg/m^3 and w/c 0.25, while the lowest compressive strength predicted was 33.72 MPa at a cement content of 689 kg/m^3 and w/c 0.29. The distribution of predicted and actual values (predictions vs. actual values) for compressive strength is displayed in Figure 4b, where the data once more follows a straight line. The predicted R^2 of 0.8729 is in reasonable agreement with the adjusted R^2 of 0.9775; i.e., the difference is less than 0.2. A_{deq} precision measures the signal-to-noise ratio. A ratio greater than four is desirable. Hence, a ratio of 28.688 indicates an adequate signal. This model can be used to navigate the design space. As shown in Figure 4c, the process order was quadratic. The perturbation plot for response 1 presented in Figure 4d revealed that all two factors have a significant influence on compressive

strength. Figure 5 displays the compressive strength of response 2 in several formats, including a 3D view, contour graph, predicted vs. actual results, and perturbation.

The equations generated from Equation (5) were used to calculate the mathematical prediction of compressive strength for response 2.

$$C.S\ for\ response\ 2 = 51.12 + 7.49\ A - 1.10\ B + 3.03\ AB - 2.18\ A^2 - 6.55\ B^2 \quad (5)$$

where A and B represent the variables (Cement and ESP).

The predicted compressive strength was 43.09, 45.93, 46.84, 45.75, 42.58, and 37.85 MPa at ESP contents of 0, 24.3, 48.6, 72.9, 97.2, and 121.5 kg/m^3, respectively, as shown in Figure 5a.

The points were far from a straight line, which indicates that the R^2 decreased significantly as shown in Figure 5b. The perturbation diagram is shown in Figure 5d to better understand the effect of cement and ESP on the compressive strength at a given point. A steep slope with an increasing trend was observed for both cement and ESP, which means that the compressive strength increased with an increase in cement and ESP. The model's F-value of 4.89 implies the model is significant. There is only a 3.04% chance that an F-value this large could occur due to noise. The *p*-values were 0.0304 less than 0.0500, which indicates that the model's terms are significant. In this case, A is a significant model term. The predicted R^2 of 0.6083 is in reasonable agreement with the adjusted R^2 of 0.6183; i.e., the difference is less than 0.1. A_{deq} precision measures the signal-to-noise ratio. A ratio greater than four is desirable. Our ratio of 7.823 indicates an adequate signal. This model can be used to navigate the design space.

Figure 6 shows, as a 3D view, response 3's compressive strength, a contour graph, predicted vs. actual results, and perturbation. The mathematical estimate of compressive strength for response 3 was computed using the equations derived from Equation (6).

$$C.S\ for\ response\ 3 = 44.33 + 7.94\ A + 0.1233\ B - 0.5375\ AB + 1.07\ A^2 - 6.95\ B^2 \quad (6)$$

where A and B represent the variables (cement and ESP).

The equation, in terms of coded factors, can be used to make predictions about the response for given levels of each factor. By default, the high levels of the factors are coded as +1 and the low levels are coded as −1. The coded equation is useful for identifying the relative impact of the factors by comparing the factor coefficients [36]. The compressive strength significantly increased at a cement content of 723 kg/m^3, with increases of 12%, 16.31%, 12.71%, and 0.72% seen for 27, 54, 81, and 108 kg/m^3 of ESP, respectively, compared to 0 ESP, as shown in Figure 6a. The model is deemed significant based on its F-value of 5.16. The probability that an F-value this great may be the result of noise is merely 2.66%. The model's terms are significant when the *p*-values are less than 0.0500, which is 0.0266 in this case. The predicted R^2 of 0.6533 is in reasonable agreement with the adjusted R^2 of 0.7035; i.e., the difference is less than 0.1, as shown in Figure 6b. As shown in Figures 6 and 7c, the process order was quadratic. As shown in Figure 6c, the highest predicted compressive strength was 59.6 MPa, and the lowest predicted compressive strength was 29.7 MPa. Figures 6 and 7d are perturbation plots, which illustrates the effect of all the design parameters at a center point in the design space.

Figure 7 displays the compressive strength for response 4 as a contour graph, a 3D view, predicted results compared to real results, and perturbation. With the equations obtained from Equation (7), the compressive strength for response 4 was mathematically estimated.

$$C.S\ for\ response\ 4 = 42.97 + 1.77\ A + 3.10\ B + 4.31\ AB + 1.42\ A^2 - 1.13\ B^2 \quad (7)$$

where A and B represent the variables (cement and WGP).

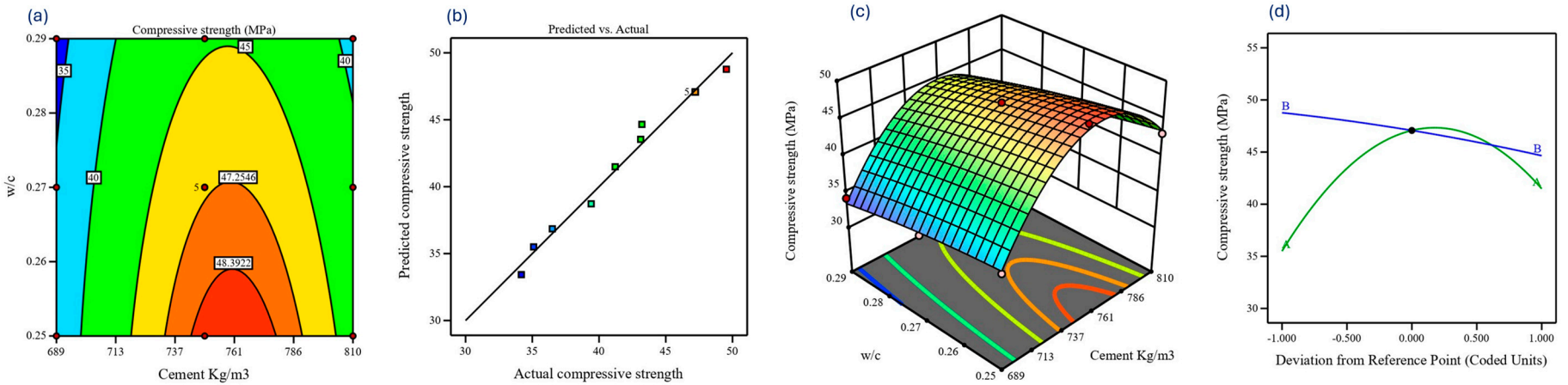

Figure 4. Response 1's compressive strength; (**a**) 3D view, (**b**) predicted vs. actual results, (**c**) contour graph, and (**d**) perturbation plot.

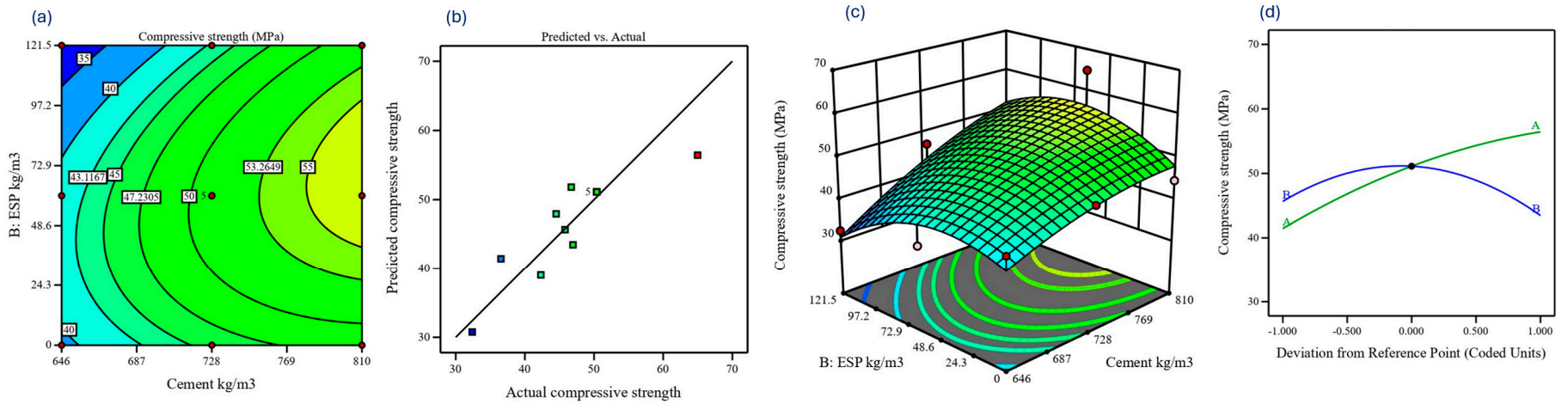

Figure 5. Response 2's compressive strength; (**a**) 3D view, (**b**) predicted vs. actual results (**c**), contour graph, and (**d**) perturbation plot.

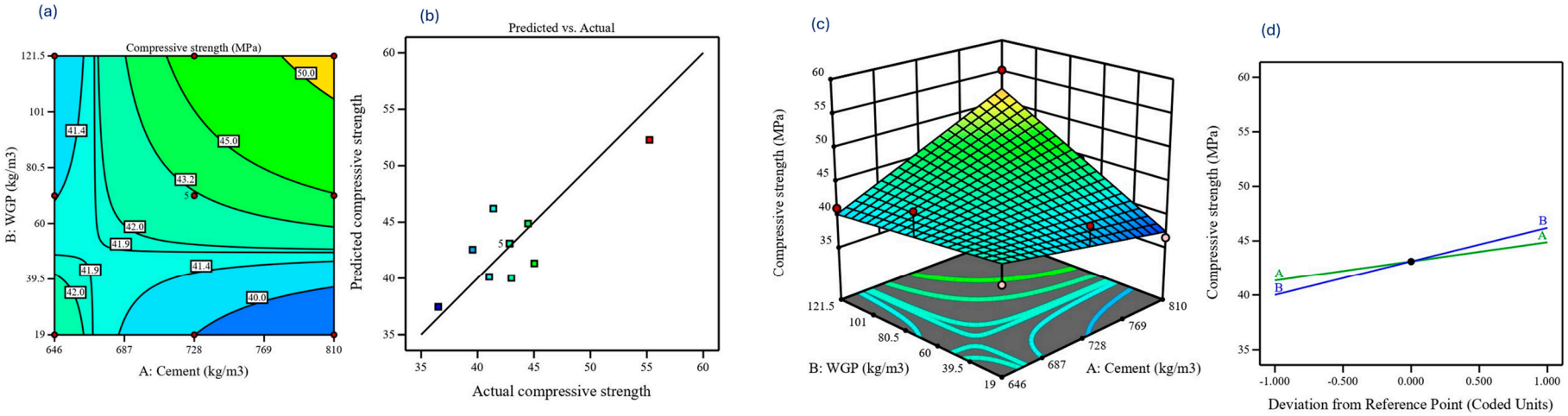

Figure 6. Response 3's compressive strength; (**a**) 3D view, (**b**) predicted vs. actual results (**c**), contour graph, and (**d**) perturbation plot.

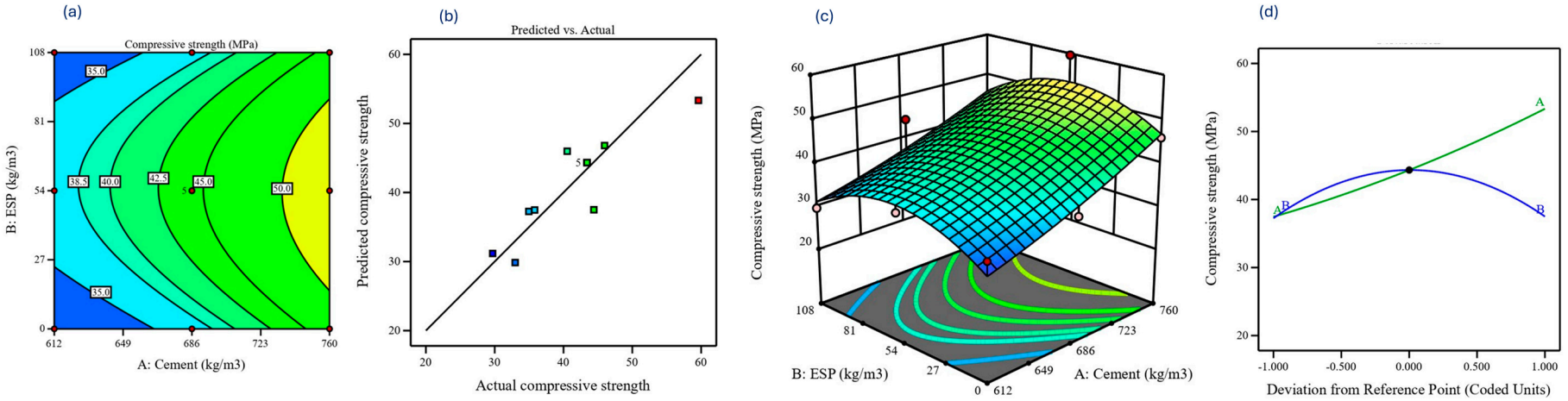

Figure 7. Response 4's compressive strength; (**a**) 3D view, (**b**) predicted vs. actual results, (**c**) contour graph, and (**d**) perturbation plot.

The model's F-value of 3.74 implies there is a 5.73% chance that an F-value this large could occur due to noise. The model's terms are considered significant when the *p*-values are less than 0.0500, and in this case, the *p*-value is 0.0473. The contour lines that followed the axes of WGP and cement were denser, as seen in Figure 7a, suggesting that the WGP and cement content have a bigger impact on compressive strength. The *p*-values are less than 0.05 when the mechanical properties are assessed using ANOVA, as demonstrated in Table 3, suggesting that the model is very significant [35,39].

Table 3. ANOVA results for the parameters of the quadratic model for the compressive strength.

Response 1						Response 2					
Source	**Sum of Squares**	**Mean Square**	**F-Value**	***p*-Value**		**Source**	**Sum of Squares**	**Mean Square**	**F-Value**	***p*-Value**	
Model	325.62	65.12	105.03	<0.0001	significant	Model	569.92	113.98	4.89	0.0304	significant
A-A	53.76	53.76	86.71	<0.0001		A-A	337.05	337.05	14.45	0.0067	
B-B	25.46	25.46	41.07	0.0004		B-B	7.22	7.22	0.3095	0.5953	
AB	0.483	0.483	0.779	0.4067		AB	36.66	36.66	1.57	0.2501	
A^2	203.35	203.35	327.97	<0.0001		A^2	13.07	13.07	0.5605	0.4785	
B^2	0.3593	0.3593	0.5795	0.4714		B^2	118.51	118.51	5.08	0.0588	
Residual	4.34	0.62				Residual	163.23	23.32			
Lack of Fit	4.34	1.45				Lack of Fit	163.23	54.41			
Std. Dev.	0.7874	Adjusted R^2	0.9775			Std. Dev.	4.83	Adjusted R^2	0.7183		
Mean	42.95	Predicted R^2	0.8729			Mean	47.09	Predicted R^2	0.7045		
C.V. %	1.83	Adeq Precision	28.688			C.V. %	10.25	Adeq Precision	7.823		
Response 3						**Response 4**					
Source	**Sum of Squares**	**Mean Square**	**F-Value**	***p*-Value**		**Source**	**Sum of Squares**	**Mean Square**	**F-Value**	***p*-Value**	
Model	520.93	104.19	5.16	0.0266	significant	Model	157.44	31.49	3.74	0.0473	significant
A-Cement	378.1	378.1	18.71	0.0035		A-Cement	18.76	18.76	2.23	0.1791	
B-ESP	0.0913	0.0913	0.0045	0.9483		B-WGP	57.6	57.6	6.84	0.0346	
AB	1.16	1.16	0.0572	0.8178		AB	74.39	74.39	8.84	0.0207	
A^2	3.17	3.17	0.1569	0.7038		A^2	5.58	5.58	0.6632	0.4423	
B^2	133.54	133.54	6.61	0.037		B^2	3.52	3.52	0.4179	0.5386	
Residual	141.45	20.21				Residual	58.91	8.42			
Lack of Fit	141.45	47.15				Lack of Fit	58.91	19.64			
Std. Dev.	4.5	R^2	0.7864			Std. Dev.	2.9	R^2	0.7277		
Mean	41.62	Adjusted R^2	0.7339			Mean	43.11	Adjusted R^2	0.6756		
C.V. %	10.8	Predicted R^2	0.6954			C.V. %	6.26	Predicted R^2	0.6512		
		Adeq Precision	7.692					Adeq Precision	9.8965		

3.2. Predicting Compressive Strength Using ANN

Using this accessible test data, a neural network model was created, trained, and evaluated. A desired artificial neural network (ANN) was constructed using a data set that included 225 data samples collected from the experimental experiments. The ANN models for compressive strength in this study were developed using a feedforward backpropagation algorithm. The modeling process utilized 70% of the 157 samples, while the testing and validation set each consisted of 15% (34 samples) of the total dataset. Feedforward backpropagation included a training function (TRAINLM), an adaptation learning function (LEARNGDM), the number of layers was 2, the number of neurons was 10, and a transfer function (TANSIG). The study allayed concerns about overfitting by proving that the accuracy gains shown in the training dataset carried over into the validation dataset [56]. Table S1 displays the MSE values for the compressive strength.

Figure 8a displays the ANN model's training state and shows that errors are repeated six times after epoch 0 and that the test ended at epoch 21. The weights from the first epoch, 0, are taken as the final weights and considered the reference point. Hence, the validation check is six since the faults occur six times before the procedure is terminated. Epoch 15 outperformed the others in the validation of the artificial neural network model, as shown by Figure 8b, with a mean squared error of 5.8901. The ability of the model to predict compressive strength with an R^2 value of 0.907 is demonstrated by the non-linear correlation between the input variables in Figure 8c. To further illustrate the difference between the real and anticipated values, Figure 8d shows the distribution of error bins.

The high proportion of the dataset falling into smaller error bins suggests that the model's predictions for concrete's compressive strength are likely quite accurate.

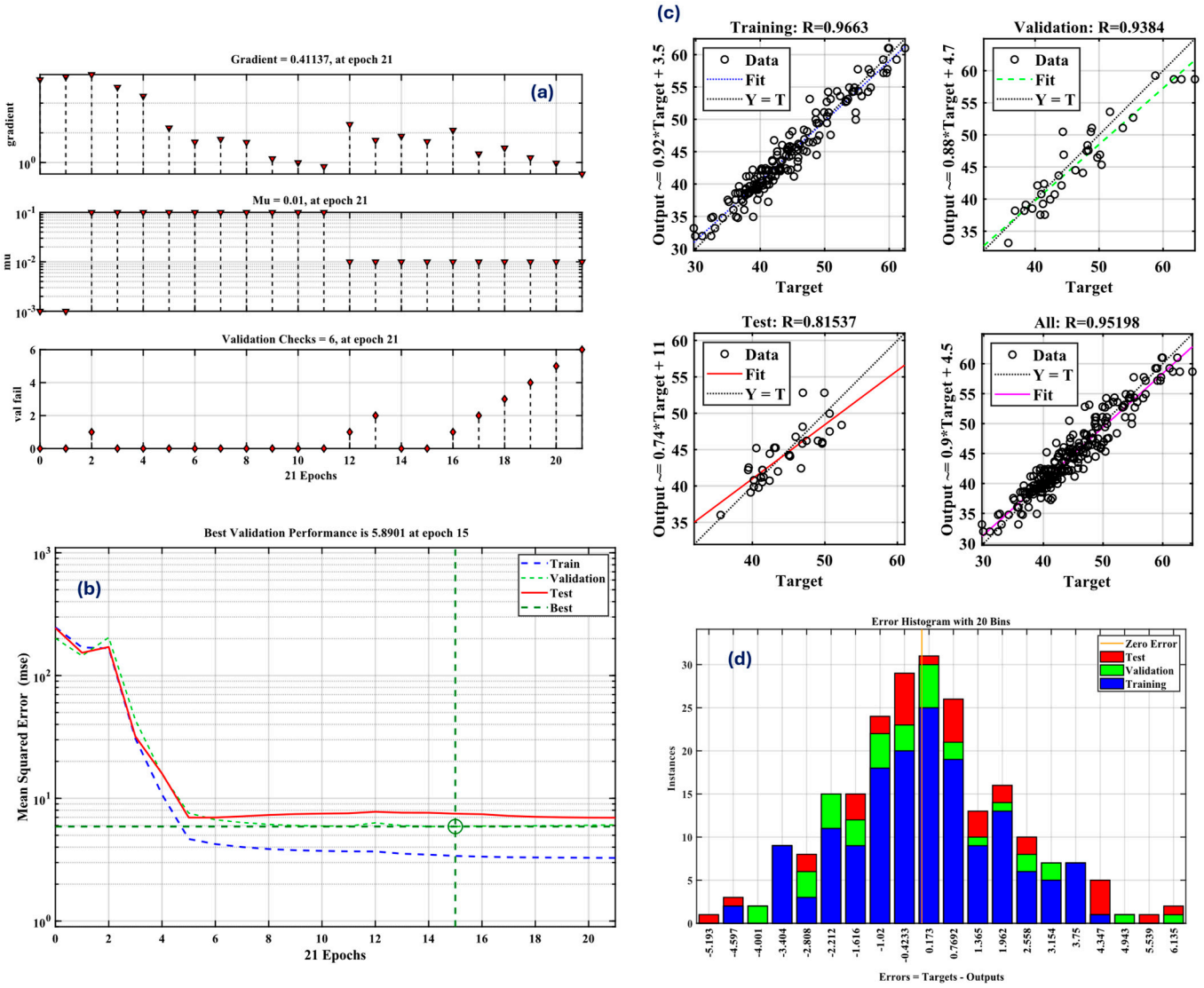

Figure 8. Features: (**a**) training state, (**b**) MSE, (**c**) R, and (**d**) error histogram of the network for compressive strength.

The absolute error distribution between the expected and experimental results is shown in Figure 9. Figure 10 shows the inputs of ANN and outputs of ANN as a Parallel Coordinates plot. An outline of the biggest inaccuracy in the ANN model may be found in this figure. The analysis of the absolute errors for CS showed that the maximum error observed was 5.97 MPa, while the lowest error seen was 5.24 MPa. According to this result, there may not be much of a difference between the targets and the predictions made using the ANN equations. Understanding that events with higher mistake frequencies are less prevalent is important.

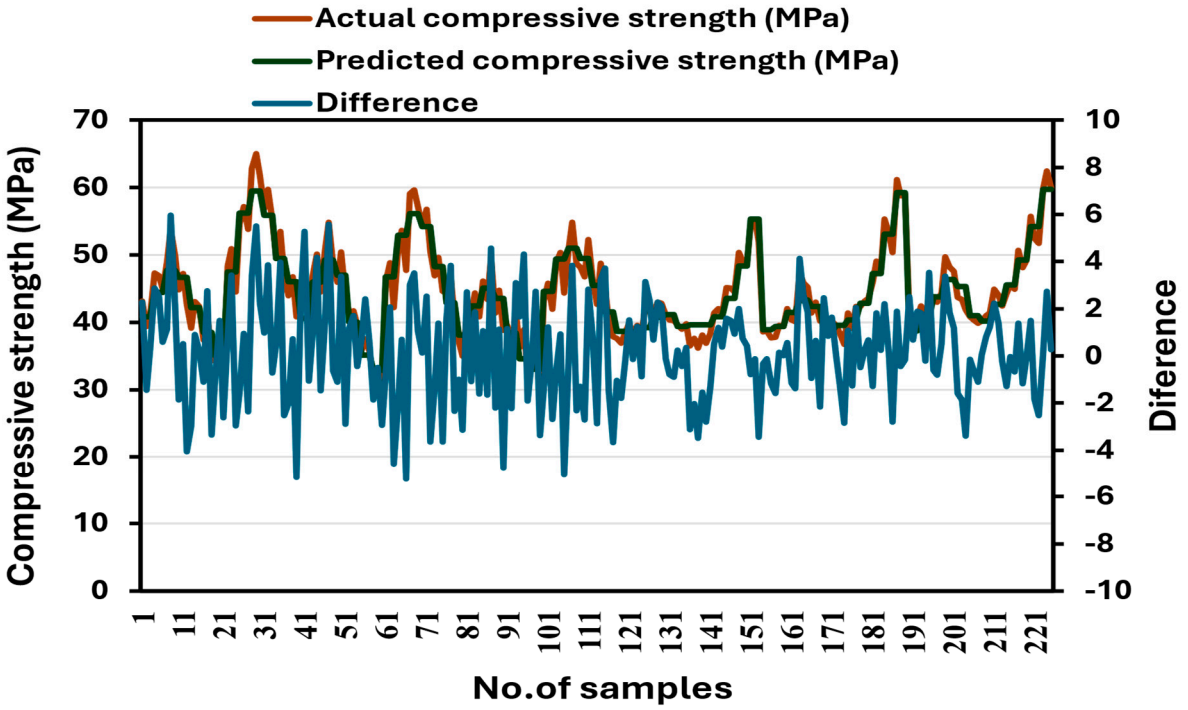

Figure 9. Distribution of experimental and ANN predicted values with difference.

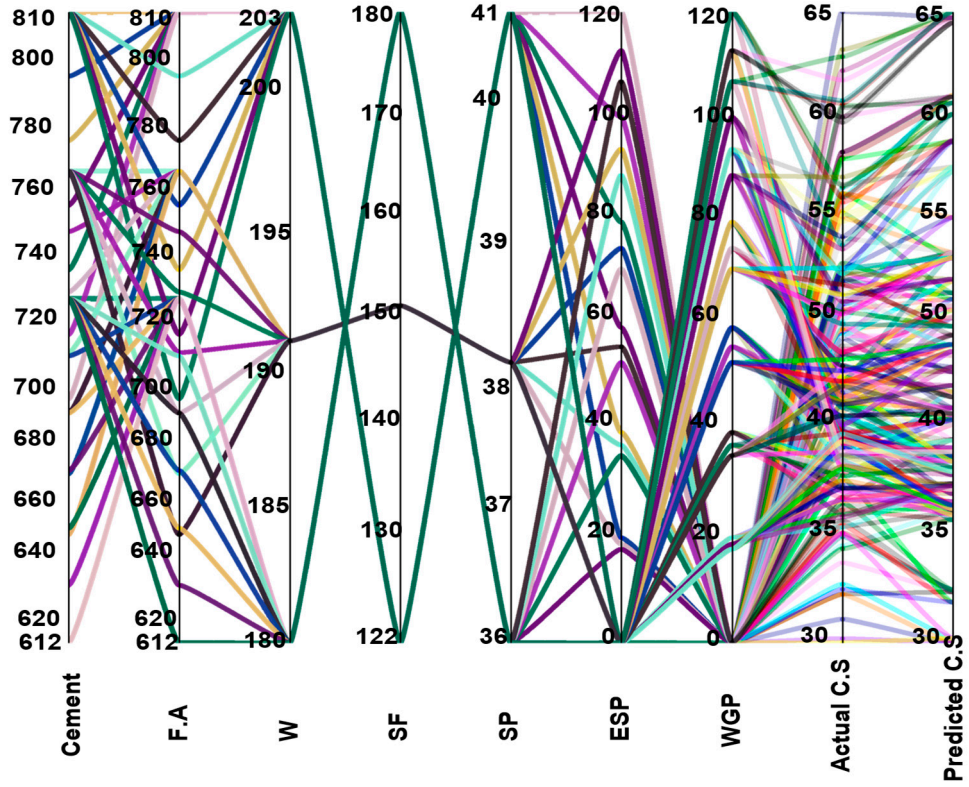

Figure 10. Parallel Coordinates plot of variables of ANN for compressive strength.

3.3. Validation of RSM and ANN in Mechanical Properties

The RSM and ANN approaches were used in this study to forecast compressive strength. ANN-based degrees of experimentation and RSM have emerged as the most widely used model and process optimization techniques in recent years [57]. We looked at the correlation between the projected and observed numbers to determine how accurate

the mathematical models were. The significant correlation confirmed that the mathematical models accurately predicted the outcomes. Table S1 displays the statistical evaluation and performance of the response surface methodology (RSM) and artificial neural network (ANN) models that were constructed. The results showed that, for both methods, the projected values of the compressive strength model agreed well with corresponding experimental values. Nevertheless, it has been observed that the RSM models for pre-designed mixes have limitations in their ability to accurately anticipate reactions when compared to artificial neural networks (ANN). The link between the expected and actual results of the RSM and ANN models was assessed using the determination coefficient (R^2) in order to verify the suitability of the finished models. Using the statistical characteristics shown in Tables 3 and S1, the created response surface method (RSM) and artificial neural network (ANN) models were assessed for correctness. Compared to the RSM techniques, the precision of the ANN-estimated R^2 was higher, and the results were significantly closer to one. As a result, the ANN-generated models demonstrated increased predictive power and accuracy. As indicated via lower MSE values which the ANN obtained in contrast to the RSM, the ANN performs better than the RSM.

4. Discussion

The current study investigated the efficacy of the ML and non-ML prediction models for assessing the compressive strength of cement concrete when ESP and WGP were used in place of some the sand and cement. There is a significant amount of waste eggshell production worldwide, most of which is dumped in landfills, endangering both human health and the environment [58]. Furthermore, the most widely used building material is cementitious composite [59–61], but its widespread use depletes natural resources and produces CO_2 [62,63]. An environmentally responsible way to replace some of the sand and cement in building materials is to use eggshell waste. Therefore, by lowering waste, preserving natural raw materials, and lowering CO_2 emissions, the use of eggshell waste in building materials will lessen its negative effects on the environment. In the same manner, the research revealed that glass has a phase and chemical composition consistent with conventional SCMs [64]. It might be of little economic worth, is plentiful, and frequently buried in land [65]. The attributes of fineness, chemical composition, and the presence of pore solution for reaction all affect the pozzolanic behavior of waste glass and the majority of pozzolans in concrete [66]. The benefits of using ESP and GWP in concrete are summarized in Figure 11.

The results mentioned above show the ability of artificial neural networks (ANN) to predict actual results, and the accuracy of the predicted results was higher than the ability of response surface methodology (RSM) to predict actual results [9]. The R^2 coefficient was the statistical measure to ensure the accuracy of the results. From the above results, it became clear that the R^2 coefficient from ANN for compressive strength exceeded 0.9, which is accurate, as shown in many previous literature [47,50,52,67], while the R^2 coefficient from RSM for compressive strength exceeded 0.8. Given the input data, the Levenberg–Marquardt (ANN) algorithm model may effectively and accurately predict the mechanical properties of concrete. The actual method is not necessary for the users to understand, which simplifies and facilitates the application [68]. Sometimes the RSM model is unable to achieve high accuracy in the predication, and this is due to the failure of the values of the variables to match the values of the RSM model, which results in low accuracy in prediction [35]. This decrease in prediction accuracy was observed. For example, the accuracy of response 1 for compressive strength was higher than the other responses, which proves that the mismatch of values between laboratory variables and model variables resulted in a decrease in prediction accuracy. To verify the efficiency of the ANN model, the model of this study was compared with the previous literature. The ANN model for this study achieved higher prediction accuracy than the ANN model for this literature [69,70]. To verify the validity of the RSM results, R^2 and p-values are looked at. If R^2 is greater than 0.8 and the p-value is less than 0.05, this proves the accuracy of the model in prediction.

The greater the R^2 than 0.8 and the lower the *p*-value than 0.05, the greater the accuracy of the predicted results [71–73].

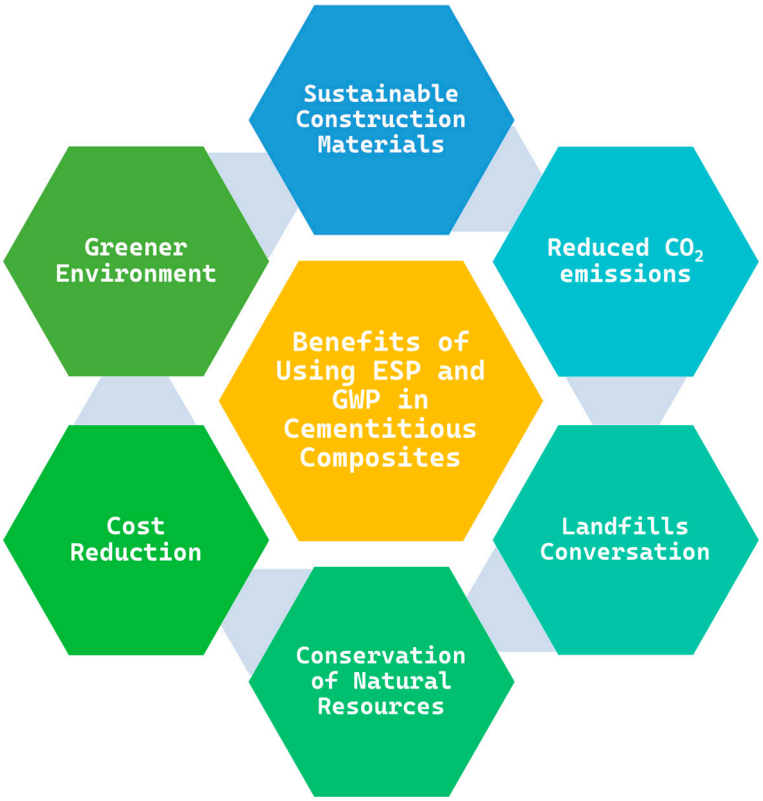

Figure 11. Utilization of ESP and WGP in concrete.

5. Conclusions

This research significantly contributes by utilizing machine learning and conventional techniques to predict the strength of waste powder additives. This study created a model that predicted compressive strength based on previous mixes, including waste components such as eggshells and glass powder additives. The investigation yielded substantial findings as follows:

- Based on the RSM analysis, the two most influential elements in predicting the compressive strength of concrete are cement and w/c ratio with R^2 0.8729.
- The RSM predicted compressive strength ranged from a maximum of 49.08 MPa at a cement content of 761 kg/m^3 and a water–cement ratio of 0.25, to a minimum of 33.72 MPa at a cement content of 689 kg/m^3 and a water–cement ratio of 0.29. The predicted compressive strength values were 43.09, 45.93, 46.84, 45.75, 42.58, and 37.85 MPa at ESP contents of 0, 24.3, 48.6, 72.9, 97.2, and 121.5 kg/m^3, respectively.
- The comparison results of the two methods show that the ANN model performs better than the RSM, with a strong correlation coefficient (R^2) of 0.907 for compressive strength.
- The maximum compressive strength predicted by the ANN model is 59.72 MPa, closely aligning with the 59.78 MPa predicted by the RSM. For the minimum compressive strength, RSM predicts a value of 22.37 MPa, whereas ANN estimates a higher value of 32.87 MPa. This comparison highlights the slight variations between the two predictive models in estimating compressive strength extremes.
- ANN and RSM models have demonstrated their effectiveness in accurately replicating the compressive characteristics of concrete.
- ANN offers the advantage of predicting multiple previous outcomes simultaneously, while RSM requires grouping prior results to enhance prediction accuracy.

- The development of these reliable predictive models (RSM and ANN) for concrete strengths incorporating ESP and WGP contributes to sustainable construction practices without performing experimental tests in the lab. In addition, it promotes waste material utilization in the field of construction materials, reducing the environmental impact of concrete production.

6. Limitations and Future Recommendations

While machine learning (ML) offers a viable means of analyzing material properties, it is not without its drawbacks. An extensive, high-quality database is essential to guarantee practical ML model training. However, acquiring a comprehensive and varied database that includes the mix composition of waste eggshell and glass powder concrete together with the corresponding compressive strength values may provide particular difficulties. The accuracy and applicability of the model may be called into question in the absence of such data. Using training data is crucial for machine learning algorithms. If the training set does not include the range of ESP and WGP-based concrete compositions or particular scenarios of interest, the predictive efficiency of the model may be reduced when making predictions for unknown mixtures or unusual processing factors. The mixture stability of ESP and GWP-based concrete is affected by a number of environmental parameters, including temperature, sample size, and moisture content. When environmental conditions or the sample shape change, it may be difficult for machine learning models built with only one set of variables to predict compressive strength. In order to calculate the compressive strength of ESP and GWP-based concrete, future research could concentrate on building an extensive database that can take into consideration the percentage of ESP and GWP, the size, shape, and composition of aggregates, as well as the dose of superplasticizer. The ESP and WGP-based cementitious composites database can be used to apply other techniques like CNN to calculate the link between input and target variables quantitatively.

Supplementary Materials: The following supporting information can be downloaded at: https://www.mdpi.com/article/10.3390/buildings14092956/s1, Table S1: Comparison of actual results with RSM and ANN predictions of compressive strength..

Author Contributions: Conceptualization, Y.G. and R.M.; Methodology, Y.G. and R.M.; Software, Y.G.; Validation, Y.G.; Formal analysis, Y.G.; Investigation, R.M.; Data curation, R.M.; Writing—original draft, Y.G.; Writing—review and editing, R.M.; Supervision, Y.G.; Project administration, R.M. All authors have read and agreed to the published version of the manuscript.

Funding: This research received no external funding.

Data Availability Statement: The data will be made available upon reasonable request from the authors.

Conflicts of Interest: There is no conflicts of interest.

References

1. Jeong, K.; Hong, T.; Kim, J. Development of a CO_2 emission benchmark for achieving the national CO_2 emission reduction target by 2030. *Energy Build.* **2018**, *158*, 86–94. [CrossRef]
2. Benhelal, E.; Zahedi, G.; Shamsaei, E.; Bahadori, A. Global strategies and potentials to curb CO_2 emissions in cement industry. *J. Clean. Prod.* **2013**, *51*, 142–161. [CrossRef]
3. Tan, H.; Du, C.; He, X.; Li, M.; Zhang, J.; Zheng, Z.; Su, Y.; Yang, J.; Deng, X.; Wang, Y. Enhancement of compressive strength of high-volume fly ash cement paste by wet grinded cement: Towards low carbon cementitious materials. *Constr. Build. Mater.* **2022**, *323*, 126458. [CrossRef]
4. Panesar, D.K.; Zhang, R. Performance comparison of cement replacing materials in concrete: Limestone fillers and supplementary cementing materials–A review. *Constr. Build. Mater.* **2020**, *251*, 118866. [CrossRef]
5. Gastaldini, A.; Hengen, M.; Gastaldini, M.; Do Amaral, F.; Antolini, M.; Coletto, T. The use of water treatment plant sludge ash as a mineral addition. *Constr. Build. Mater.* **2015**, *94*, 513–520. [CrossRef]
6. Khan, M.; McNally, C. Recent developments on low carbon 3D printing concrete: Revolutionizing construction through innovative technology. *Clean. Mater.* **2024**, *12*, 100251. [CrossRef]
7. Malhotra, V. Introduction: Sustainable development and concrete technology. *Concr. Int.* **2002**, *24*, 22.

8. Ali, M.; Saidur, R.; Hossain, M. A review on emission analysis in cement industries. *Renew. Sustain. Energy Rev.* **2011**, *15*, 2252–2261. [CrossRef]
9. Hammoudi, A.; Moussaceb, K.; Belebchouche, C.; Dahmoune, F. Comparison of artificial neural network (ANN) and response surface methodology (RSM) prediction in compressive strength of recycled concrete aggregates. *Constr. Build. Mater.* **2019**, *209*, 425–436. [CrossRef]
10. Ejaz, N.; Akhtar, N.; Hashmi, H.; Naeem, U.A. Environmental impacts of improper solid waste management in developing countries: A case study of Rawalpindi city. *Sustain. World* **2010**, *142*, 379–387.
11. Jayasankar, R.; Mahindran, N.; Ilangovan, R. Studies on concrete using fly ash, rice husk ash and egg shell powder. *Int. J. Civ. Struct. Eng.* **2010**, *1*, 362–372.
12. Sathiparan, N. Utilization prospects of eggshell powder in sustainable construction material–A review. *Constr. Build. Mater.* **2021**, *293*, 123465. [CrossRef]
13. Oliveira, D.A.; Benelli, P.; Amante, E.R. A literature review on adding value to solid residues: Egg shells. *J. Clean. Prod.* **2013**, *46*, 42–47. [CrossRef]
14. Laca, A.; Laca, A.; Díaz, M. Eggshell waste as catalyst: A review. *J. Environ. Manag.* **2017**, *197*, 351–359. [CrossRef]
15. Shiferaw, N.; Habte, L.; Thenepalli, T.; Ahn, J.W. Effect of eggshell powder on the hydration of cement paste. *Materials* **2019**, *12*, 2483. [CrossRef]
16. Guan, J.; Liu, L.; Li, L.; Xie, C.; Khan, M. Mesoscopic model for the fracture of polymethyl methacrylate bone cement. *Eng. Fract. Mech.* **2024**, *303*, 110085. [CrossRef]
17. Chandrasekaran, V.; Vasanth, M.; Thirunavukkarasu, S. Experimental investigation of partial replacement of cement with glass powder and eggshell powder ash in concrete. *Civ. Eng. Res. J.* **2018**, *5*, 555662. [CrossRef]
18. Mehta, A.; Ashish, D.K. Silica fume and waste glass in cement concrete production: A review. *J. Build. Eng.* **2020**, *29*, 100888. [CrossRef]
19. Jiang, X.; Xiao, R.; Bai, Y.; Huang, B.; Ma, Y. Influence of waste glass powder as a supplementary cementitious material (SCM) on physical and mechanical properties of cement paste under high temperatures. *J. Clean. Prod.* **2022**, *340*, 130778. [CrossRef]
20. Bilondi, M.P.; Toufigh, M.M.; Toufigh, V. Experimental investigation of using a recycled glass powder-based geopolymer to improve the mechanical behavior of clay soils. *Constr. Build. Mater.* **2018**, *170*, 302–313. [CrossRef]
21. Xiao, R.; Polaczyk, P.; Zhang, M.; Jiang, X.; Zhang, Y.; Huang, B.; Hu, W. Evaluation of glass powder-based geopolymer stabilized road bases containing recycled waste glass aggregate. *Transp. Res. Rec.* **2020**, *2674*, 22–32. [CrossRef]
22. Shi, C.; Wu, Y.; Riefler, C.; Wang, H. Characteristics and pozzolanic reactivity of glass powders. *Cem. Concr. Res.* **2005**, *35*, 987–993. [CrossRef]
23. ASTM International. *Standard Specification for Coal Fly Ash and Raw or Calcined Natural Pozzolan for Use in Concrete*; ASTM International: West Conshohocken, PA, USA, 2012; p. 4.
24. Aliabdo, A.A.; Abd Elmoaty, M.; Aboshama, A.Y. Utilization of waste glass powder in the production of cement and concrete. *Constr. Build. Mater.* **2016**, *124*, 866–877. [CrossRef]
25. Golafshani, E.M.; Behnood, A.; Arashpour, M. Predicting the compressive strength of normal and High-Performance Concretes using ANN and ANFIS hybridized with Grey Wolf Optimizer. *Constr. Build. Mater.* **2020**, *232*, 117266. [CrossRef]
26. Foucquier, A.; Robert, S.; Suard, F.; Stéphan, L.; Jay, A. State of the art in building modelling and energy performances prediction: A review. *Renew. Sustain. Energy Rev.* **2013**, *23*, 272–288. [CrossRef]
27. Song, H.; Ahmad, A.; Farooq, F.; Ostrowski, K.A.; Maślak, M.; Czarnecki, S.; Aslam, F. Predicting the compressive strength of concrete with fly ash admixture using machine learning algorithms. *Constr. Build. Mater.* **2021**, *308*, 125021. [CrossRef]
28. Haykin, S. *Neural Networks and Learning Machines, 3/E*; Pearson Education India: Hoboken, NJ, USA, 2009.
29. Rahman, A.A.; Zhang, X. Prediction of oscillatory heat transfer coefficient for a thermoacoustic heat exchanger through artificial neural network technique. *Int. J. Heat Mass Transf.* **2018**, *124*, 1088–1096. [CrossRef]
30. Ford, E.; Kailas, S.; Maneparambil, K.; Neithalath, N. Machine learning approaches to predict the micromechanical properties of cementitious hydration phases from microstructural chemical maps. *Constr. Build. Mater.* **2020**, *265*, 120647. [CrossRef]
31. Lau, C.K.; Lee, H.; Vimonsatit, V.; Huen, W.Y.; Chindaprasirt, P. Abrasion resistance behaviour of fly ash based geopolymer using nanoindentation and artificial neural network. *Constr. Build. Mater.* **2019**, *212*, 635–644. [CrossRef]
32. Konstantopoulos, G.; Koumoulos, E.P.; Charitidis, C.A. Testing novel portland cement formulations with carbon nanotubes and intrinsic properties revelation: Nanoindentation analysis with machine learning on microstructure identification. *Nanomaterials* **2020**, *10*, 645. [CrossRef]
33. Adhikary, B.B.; Mutsuyoshi, H. Prediction of shear strength of steel fiber RC beams using neural networks. *Constr. Build. Mater.* **2006**, *20*, 801–811. [CrossRef]
34. Cook, R.; Lapeyre, J.; Ma, H.; Kumar, A. Prediction of compressive strength of concrete: Critical comparison of performance of a hybrid machine learning model with standalone models. *J. Mater. Civ. Eng.* **2019**, *31*, 04019255. [CrossRef]
35. Ferdosian, I.; Camões, A. Eco-efficient ultra-high performance concrete development by means of response surface methodology. *Cem. Concr. Compos.* **2017**, *84*, 146–156. [CrossRef]
36. Desai, K.M.; Survase, S.A.; Saudagar, P.S.; Lele, S.; Singhal, R.S. Comparison of artificial neural network (ANN) and response surface methodology (RSM) in fermentation media optimization: Case study of fermentative production of scleroglucan. *Biochem. Eng. J.* **2008**, *41*, 266–273. [CrossRef]

37. Esfahanian, M.; Nikzad, M.; Najafpour, G.; Ghoreyshi, A.A. Modeling and optimization of ethanol fermentation using Saccharomyces cerevisiae: Response surface methodology and artificial neural network. *Chem. Ind. Chem. Eng. Q.* **2013**, *19*, 241–252. [CrossRef]
38. Hasan, M.M.; Kabir, A. Prediction of compressive strength of concrete from early age test result. In Proceedings of the 4th Annual Paper Meet and 1st Civil Engineering Congress, Dhaka, Bangladesh, 22–24 December 2011; Volume 2011, pp. 978–984.
39. Ali, M.; Kumar, A.; Yvaz, A.; Salah, B. Central composite design application in the optimization of the effect of pumice stone on lightweight concrete properties using RSM. *Case Stud. Constr. Mater.* **2023**, *18*, e01958. [CrossRef]
40. Grabiec, A.M.; Piasta, Z. Study on compatibility of cement–superplasticiser assisted by multicriteria statistical optimisation. *J. Mater. Process. Technol.* **2004**, *152*, 197–203. [CrossRef]
41. Mandal, A.; Roy, P. Modeling the compressive strength of molasses–cement sand system using design of experiments and back propagation neural network. *J. Mater. Process. Technol.* **2006**, *180*, 167–173. [CrossRef]
42. Nambiar, E.K.; Ramamurthy, K. Models relating mixture composition to the density and strength of foam concrete using response surface methodology. *Cem. Concr. Compos.* **2006**, *28*, 752–760. [CrossRef]
43. Khan, K.; Ahmad, W.; Amin, M.N.; Rafiq, M.I.; Arab, A.M.A.; Alabdullah, I.A.; Alabduljabbar, H.; Mohamed, A. Evaluating the effectiveness of waste glass powder for the compressive strength improvement of cement mortar using experimental and machine learning methods. *Heliyon* **2023**, *9*, e16288. [CrossRef]
44. Alsharari, F.; Khan, K.; Amin, M.N.; Ahmad, W.; Khan, U.; Mutnbak, M.; Houda, M.; Yosri, A.M. Sustainable use of waste eggshells in cementitious materials: An experimental and modeling-based study. *Case Stud. Constr. Mater.* **2022**, *17*, e01620. [CrossRef]
45. Gallo, C. Artificial neural networks tutorial. In *Encyclopedia of Information Science and Technology*, 3rd ed.; IGI Global: Hershey, PA, USA, 2015; pp. 6369–6378.
46. Schilling, A.; Maier, A.; Gerum, R.; Metzner, C.; Krauss, P. Quantifying the separability of data classes in neural networks. *Neural Netw.* **2021**, *139*, 278–293. [CrossRef] [PubMed]
47. Güçlüer, K.; Özbeyaz, A.; Göymen, S.; Günaydın, O. A comparative investigation using machine learning methods for concrete compressive strength estimation. *Mater. Today Commun.* **2021**, *27*, 102278. [CrossRef]
48. Muñoz-Zavala, A.E.; Macías-Díaz, J.E.; Alba-Cuéllar, D.; Guerrero-Díaz-de-León, J.A. A Literature Review on Some Trends in Artificial Neural Networks for Modeling and Simulation with Time Series. *Algorithms* **2024**, *17*, 76. [CrossRef]
49. Khandelwal, M.; Singh, T. Prediction of macerals contents of Indian coals from proximate and ultimate analyses using artificial neural networks. *Fuel* **2010**, *89*, 1101–1109. [CrossRef]
50. Singh, T.; Kanchan, R.; Verma, A.; Saigal, K. A comparative study of ANN and neuro-fuzzy for the prediction of dynamic constant of rockmass. *J. Earth Syst. Sci.* **2005**, *114*, 75–86. [CrossRef]
51. Lippmann, R.P. An introduction to computing with neural nets. *ACM SIGARCH Comput. Archit. News* **1988**, *16*, 7–25. [CrossRef]
52. Kewalramani, M.A.; Gupta, R. Concrete compressive strength prediction using ultrasonic pulse velocity through artificial neural networks. *Autom. Constr.* **2006**, *15*, 374–379. [CrossRef]
53. Habibi, A.; Ramezanianpour, A.M.; Mahdikhani, M.; Bamshad, O. RSM-based evaluation of mechanical and durability properties of recycled aggregate concrete containing GGBFS and silica fume. *Constr. Build. Mater.* **2021**, *270*, 121431. [CrossRef]
54. Luthfi, N.; Fukushima, T.; Wang, X.; Takisawa, K. Significance and Optimization of Operating Parameters in Hydrothermal Carbonization Using RSM–CCD. *Thermo* **2024**, *4*, 82–99. [CrossRef]
55. Ofuyatan, O.M.; Agbawhe, O.B.; Omole, D.O.; Igwegbe, C.A.; Ighalo, J.O. RSM and ANN modelling of the mechanical properties of self-compacting concrete with silica fume and plastic waste as partial constituent replacement. *Clean. Mater.* **2022**, *4*, 100065. [CrossRef]
56. Khan, A.Q.; Awan, H.A.; Rasul, M.; Siddiqi, Z.A.; Pimanmas, A. Optimized artificial neural network model for accurate prediction of compressive strength of normal and high strength concrete. *Clean. Mater.* **2023**, *10*, 100211. [CrossRef]
57. Dahmoune, F.; Remini, H.; Dairi, S.; Aoun, O.; Moussi, K.; Bouaoudia-Madi, N.; Adjeroud, N.; Kadri, N.; Lefsih, K.; Boughani, L. Ultrasound assisted extraction of phenolic compounds from P. lentiscus L. leaves: Comparative study of artificial neural network (ANN) versus degree of experiment for prediction ability of phenolic compounds recovery. *Ind. Crops Prod.* **2015**, *77*, 251–261. [CrossRef]
58. Yang, D.; Zhao, J.; Ahmad, W.; Amin, M.N.; Aslam, F.; Khan, K.; Ahmad, A. Potential use of waste eggshells in cement-based materials: A bibliographic analysis and review of the material properties. *Constr. Build. Mater.* **2022**, *344*, 128143. [CrossRef]
59. Khan, U.A.; Jahanzaib, H.M.; Khan, M.; Ali, M. Improving the tensile energy absorption of high strength natural fiber reinforced concrete with fly-ash for bridge girders. *Key Eng. Mater.* **2018**, *765*, 335–342. [CrossRef]
60. Farooqi, M.U.; Ali, M. Durability evaluation of wheat straw reinforced concrete for sustainable structures. *J. Build. Eng.* **2024**, *82*, 108400. [CrossRef]
61. Akbulut, Z.F.; Guler, S.; Osmanoğlu, F.; Kıvanç, M.R.; Khan, M. Evaluating sustainable colored mortars reinforced with fly ash: A comprehensive study on physical and mechanical properties under high-temperature exposure. *Buildings* **2024**, *14*, 453. [CrossRef]
62. Li, G.; Zhou, C.; Ahmad, W.; Usanova, K.I.; Karelina, M.; Mohamed, A.M.; Khallaf, R. Fly ash application as supplementary cementitious material: A review. *Materials* **2022**, *15*, 2664. [CrossRef]

63. Ahmed, T.; Farooqi, M.; Ali, M. Compressive behavior of rice straw-reinforced concrete for rigid pavements. *IOP Conf. Ser. Mater. Sci. Eng.* **2020**, *770*, 012004. [CrossRef]
64. Soroushian, P. Strength and durability of recycled aggregate concrete containing milled glass as partial replacement for cement. *Constr. Build. Mater.* **2012**, *29*, 368–377.
65. Byars, E.; Zhu, H.; Meyer, C. Use of waste glass for construction products: Legislative and technical issues. In *Recycling and Reuse of Waste Materials*; Thomas Telford Publishing: London, UK, 2003; pp. 827–838.
66. Rashad, A.M. A brief on high-volume Class F fly ash as cement replacement–A guide for Civil Engineer. *Int. J. Sustain. Built Environ.* **2015**, *4*, 278–306. [CrossRef]
67. Bilim, C.; Atiş, C.D.; Tanyildizi, H.; Karahan, O. Predicting the compressive strength of ground granulated blast furnace slag concrete using artificial neural network. *Adv. Eng. Softw.* **2009**, *40*, 334–340. [CrossRef]
68. Feng, D.-C.; Liu, Z.-T.; Wang, X.-D.; Chen, Y.; Chang, J.-Q.; Wei, D.-F.; Jiang, Z.-M. Machine learning-based compressive strength prediction for concrete: An adaptive boosting approach. *Constr. Build. Mater.* **2020**, *230*, 117000. [CrossRef]
69. Amiri, M.; Hatami, F. Prediction of mechanical and durability characteristics of concrete including slag and recycled aggregate concrete with artificial neural networks (ANNs). *Constr. Build. Mater.* **2022**, *325*, 126839. [CrossRef]
70. Bonagura, M.; Nobile, L. Artificial neural network (ANN) approach for predicting concrete compressive strength by SonReb. *Struct. Durab. Health Monit.* **2021**, *15*, 125–137. [CrossRef]
71. Ghafari, E.; Costa, H.; Júlio, E. RSM-based model to predict the performance of self-compacting UHPC reinforced with hybrid steel micro-fibers. *Constr. Build. Mater.* **2014**, *66*, 375–383. [CrossRef]
72. Li, Q.; Cai, L.; Fu, Y.; Wang, H.; Zou, Y. Fracture properties and response surface methodology model of alkali-slag concrete under freeze–thaw cycles. *Constr. Build. Mater.* **2015**, *93*, 620–626. [CrossRef]
73. Alyamac, K.E.; Ghafari, E.; Ince, R. Development of eco-efficient self-compacting concrete with waste marble powder using the response surface method. *J. Clean. Prod.* **2017**, *144*, 192–202. [CrossRef]